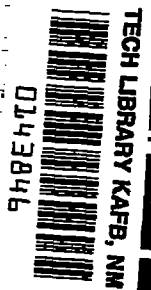


NACA RM No. L8H23

RM L8H23

RM No. L8H23



RESEARCH MEMORANDUM

EXPERIMENTAL DETERMINATION OF THE LATERAL STABILITY OF A
GLIDER TOWED BY A SINGLE TOWLINE AND CORRELATION WITH
AN APPROXIMATE THEORY

By

Bernard Maggin and Robert E. Shanks

Langley Aeronautical Laboratory
Langley Field, Va.

AFMDC
LIBRARY
- 2811

NATIONAL ADVISORY COMMITTEE
FOR AERONAUTICS

WASHINGTON
November 12, 1948

7147

555

319.98/12



RESEARCH MEMORANDUM

EXPERIMENTAL DETERMINATION OF THE LATERAL STABILITY OF A
GLIDER TOWED BY A SINGLE TOWLINE AND CORRELATION WITH
AN APPROXIMATE THEORY

By Bernard Maggin and Robert E. Shanks

SUMMARY

An experimental investigation was made to determine the effects of various design parameters on the lateral-stability characteristics of a glider towed by a single towline. The investigation showed that it is possible to obtain inherent lateral stability with a single towline system.

An approximate theoretical analysis was also made and the results of calculations made by use of this analysis were compared with the model flight-test results. Although the theoretical damping results are too conservative to be of much practical value, the existence of divergences and the periods of the lateral oscillations are predicted with fair accuracy.

INTRODUCTION

The Army and Navy have long been interested in towed gliders as a means of transporting men, material, aerial targets or guided missiles. One of the major problems connected with the use of towed gliders has been that of obtaining lateral stability of the glider on tow. Once trim conditions had been established, an inherently stable glider towline system would require no pilot attention and thus glider-pilot fatigue would be reduced on long flights or under conditions of poor visibility. In addition, it would make feasible some glider applications that are now impractical.

In order to obtain lateral stability, various automatic and semi-automatic devices have been used but these devices are limited in their application by their complexity and maintenance problems. Glider-position indicators, as a visual aid to the pilot during blind-flying conditions, have proved unsatisfactory. Various systems other than a single line have been proposed. One such system consisting of twin parallel towlines was studied in a theoretical and experimental investigation in the Langley free-flight tunnel (references 1 and 2). In general, however, it appears that the most satisfactory solution to the towed-glider problem would be an inherently stable single-towline system.

Although a considerable amount of experimental and theoretical work has been conducted in this country and by the British, to date no satisfactory theory predicting the lateral-stability characteristics of a glider on a single towline has been reported.

The results of an experimental investigation to determine the effect of varying the effective dihedral, directional stability, relative density, towline attachment point, and towline length are given in the present report. In addition, a simplified theoretical method developed to determine the lateral-stability characteristics of a glider towed by a single towline is presented in the appendix and the results of calculations made by this theory are compared with the experimental data.

S Y M B O L S

The forces and moments are referred to the stability axes (see fig. 1) unless otherwise stated. These axes are defined as an orthogonal system having its origin at the center of gravity and in which the Z-axis is in the plane of symmetry and perpendicular to the relative wind, the X-axis is in the plane of symmetry and perpendicular to the Z-axis, and the Y-axis is perpendicular to the plane of symmetry. The coefficients presented here refer to the glider except where otherwise noted.

W	weight, pounds
m	mass, slugs
b	wing span at zero dihedral angle, feet
D	drag, pounds; differential operator (d/ds)
L	lift, pounds; rolling moment about the X stability axis, foot-pounds
M	pitching moment about the Y stability axis, foot-pounds
N	yawing moment about the Z stability axis, foot-pounds
C_L	lift coefficient ($Lift/qS$)
C_D	drag coefficient ($Drag/qS$)
C_Y	lateral-force coefficient (Y/qS)
C_W	weight coefficient (W/qS)
C_l	rolling-moment coefficient (L/qSb)

C_m	pitching-moment coefficient ($M/qS\bar{c}$)
C_n	yawing-moment coefficient (N/qSb)
ψ	angle of yaw, radians
ψ'	angle between X-axis and projection of the towline on the X-Y plane
β	angle of sideslip, radians
ϕ	angle of bank, radians
ϕ'	angle between Z-axis and projection of the towline on the Y-Z plane
p	rolling angular velocity, radians per second
r	yawing angular velocity, radians per second
ϵ	angle between towline and the relative wind, degrees
α	angle of attack, measured from the top of the boom to the relative wind, degrees
α_0	angle of attack; measured from the angle of zero lift, degrees
Γ	wing dihedral angle (positive wing tips up), degrees
L_β	rate of change of rolling moment with angle of sideslip ($\partial L/\partial \beta$)
L_p	rate of change of rolling moment with rolling velocity ($\partial L/\partial p$)
L_r	rate of change of rolling moment with yawing velocity ($\partial L/\partial r$)
N_β	rate of change of yawing moment with angle of sideslip ($\partial N/\partial \beta$)
\bar{c}	mean aerodynamic chord of wing, feet
S	wing area, square feet
S_t	vertical-tail area, square feet
t	time, seconds
ρ	mass density of air, slugs per cubic foot
q	dynamic pressure, pounds per square foot $\left(\frac{1}{2}\rho V^2\right)$

g	gravitational acceleration, ft/sec ²
μ	relative-density factor $\left(\frac{m}{\rho S b}\right)$
k_X	radius of gyration about X-axis, feet
k_Z	radius of gyration about Z-axis, feet
K_X	radius of gyration about X-axis, spans
K_Z	radius of gyration about Z-axis, spans
K_{X_p}	radius of gyration about principal longitudinal axis, spans
K_{Z_p}	radius of gyration about principal normal axis, spans
K_{XZ}	product-of-inertia factor, spans ² $\left(K_{Z_p}^2 - K_{X_p}^2\right) \cos \eta \sin \eta$
η	angle of attack of principal longitudinal axis of airplane; positive when forward end of major principal axis is above X-axis, see figure 1
x	distance along X-axis from center of gravity of glider to the towline attachment point, spans
z	distance along Z-axis from center of gravity of glider to the towline attachment point, spans
y	sidewise movement of center of gravity along Y-axis, feet, see figure 8
y'	sidewise movement of center of gravity along Y-axis, spans
l	towline length, spans
V	true airspeed, feet per second
v	velocity along Y-axis, feet per second
T	towline tension, pounds
Y	lateral force, pounds

$C_{Y\beta}$ rate of change of lateral-force coefficient with angle of sideslip, per radian $\left(\frac{\partial C_Y}{\partial \beta}\right)$

$C_{l\beta}$ rate of change of rolling-moment coefficient with angle of sideslip, per radian $(\partial C_l / \partial \beta)$

C_{lp} rate of change of rolling-moment coefficient with rolling angular velocity factor $\left(\frac{\partial C_l}{\partial \frac{pb}{2V}}\right)$

C_{lr} rate of change of rolling-moment coefficient with yawing velocity factor $\left(\frac{\partial C_l}{\partial \frac{rb}{2V}}\right)$

$C_{n\beta}$ rate of change of yawing-moment coefficient with angle of sideslip, per radian $\left(\frac{\partial C_n}{\partial \beta}\right)$

C_{np} rate of change of yawing-moment coefficient with rolling angular velocity factor $\left(\frac{\partial C_n}{\partial \frac{pb}{2V}}\right)$

C_{nr} rate of change of yawing-moment coefficient with yawing angular velocity factor $\left(\frac{\partial C_n}{\partial \frac{rb}{2V}}\right)$

A, B, C, E, F, G, H, I, J, K coefficients of the stability equation

P period of oscillation, seconds

$T_{\frac{1}{2}}$ time required for a motion to damp to one-half amplitude

id imaginary portion of complex root

c real portion of complex root or a real root

Towline terms:

Y_y rate of change of the lateral force with sidewise displacement $(\partial Y / \partial y)$

Y_ψ rate of change of lateral force with angle of yaw $(\partial Y / \partial \psi)$

Y_ϕ rate of change of lateral force with angle of bank $(\partial Y / \partial \phi)$

L_y	rate of change of rolling moment with sidewise displacement ($\partial L/\partial y$)
L_ψ	rate of change of rolling moment with angle of yaw ($\partial L/\partial \psi$)
L_ϕ	rate of change of rolling moment with angle of bank ($\partial L/\partial \phi$)
N_y	rate of change of yawing moment with sidewise displacement ($\partial N/\partial y$)
N_ψ	rate of change of yawing moment with angle of yaw ($\partial N/\partial \psi$)
N_ϕ	rate of change of yawing moment with angle of bank ($\partial N/\partial \phi$)
T_{yy}'	rate of change of lateral force caused by towline tension with sidewise displacement ($\partial T_y/\partial y'$)
$T_{y\psi}$	rate of change of lateral force caused by towline tension with angle of yaw ($\partial T_y/\partial \psi$)
$T_{y\phi}$	rate of change of lateral force caused by towline tension with angle of bank ($\partial T_y/\partial \phi$)
T_{ny}'	rate of change of yawing moment caused by towline tension with sidewise displacement ($\partial T_n/\partial y'$)
$T_{n\psi}$	rate of change of yawing moment caused by towline tension with angle of yaw ($\partial T_n/\partial \psi$)
$T_{n\phi}$	rate of change of yawing moment caused by towline tension with angle of bank ($\partial T_n/\partial \phi$)
T_{ly}'	rate of change of rolling moment caused by towline tension with sidewise displacement ($\partial T_l/\partial y'$)
$T_{l\psi}$	rate of change of rolling moment caused by towline tension with angle of yaw ($\partial T_l/\partial \psi$)
$T_{l\phi}$	rate of change of rolling moment caused by towline tension with angle of roll ($\partial T_l/\partial \phi$)

T E S T S

APPARATUS

All the tow tests of the model were conducted in the Langley free-flight tunnel, a complete description of which is given in reference 3. Photographs of the model mounted on a stand and on tow in the tunnel are presented in figure 2.

A sketch of the model used in the tests is presented in figure 3. The model consisted of a wooden boom upon which the wing and stabilizing surfaces were mounted. A Rhode St. Genese 35 airfoil section was used in accordance with free-flight-tunnel practice of using airfoil sections that give maximum lift coefficients in low-scale tests approximately equal to those obtained in full-scale tests of conventional airfoil sections. The stabilizing surfaces were constructed of $\frac{1}{8}$ -inch sheet balsa.

The wings were mounted so that a range of geometric dihedral angles between -5° and 15° could be obtained, and the model was arranged to allow for mounting of any one of three vertical tails, 5 percent, 7.5 percent, and 10 percent of the wing area. (See fig. 3.)

The glider model was equipped with conventional control surfaces actuated by a pilot through standard free-flight-tunnel control mechanisms. A complete description of the flight models and flight technique used in free-flight-tunnel testing is given in reference 3.

The model photograph and sketch in figures 2 and 3, respectively, show the special tow bar used on the model. The tow bar consisted of a horizontal bar mounted on two vertical bars, one located in the nose of the model, the other at about the 60-percent station of the root chord of the wing. The vertical position of the horizontal bar could be varied and the towline attachment could be made anywhere along the horizontal bar. The tow bar was used for convenience, but in practice a trifurcated bridle system, which gives, in effect, a fixed attachment point at the apex of the glider bridle lines could be used, provided that the attachment lines remain in tension. Figure 4 shows some of the more commonly used single-towline attachment systems. From a study of these systems it can be seen that the tow-bar arrangement used in the tests can represent any of these common systems insofar as the towline attachment point is concerned if the longitudinal trim is assumed not to change (as is approximately the case) during a disturbance.

The relative density μ of the model was adjusted without changing the moments of inertia by adding weights at the model center of gravity. Increasing the value of μ in this manner decreased the radii of gyration as shown in table I.

METHOD

In the tests the airspeed was held constant and the trim angle of the elevator was adjusted to obtain approximately the desired angle of attack and towline angle. The model was controlled by the pilot who, in the case of stable tow configurations, supplied disturbances to start an oscillation. In the case of unstable tow configurations, the pilot steadied the model so that the oscillation could develop from the steady state and then could be stopped when sufficient records of the motion had been obtained. During the oscillation the controls were fixed.

The motions of the model for the various test conditions were recorded by two motion-picture cameras, one mounted on top of the tunnel directly above the glider model, the other at the rear of the tunnel directly behind the model. In some instances the period of the lateral motion was measured with a stop watch. For each tow condition the towline angle and angle of attack were measured visually with a protractor mounted at the side of the tunnel.

From the motion-picture records, plots were made of the sidewise displacement, angle of bank, and angle of yaw against time for the conditions tested. From these records the period and time to damp to one-half amplitude of the lateral oscillations were obtained. Some representative flight records are presented in figures 5(a) and 5(b).

SCOPE

A list of the conditions covered in the tests is presented in table II. It will be noted that the tow attachment points considered are above and forward of the glider center of gravity and the glider is below and behind the tug. These glider tug configurations were used because past towing experience indicated that they would be best from the standpoint of obtaining lateral stability on tow. This table shows the effects on lateral stability of varying the effective dihedral, directional stability, relative density, towline attachment point, and towline length. In order to determine the effects of these parameters,

they were varied one at a time from a basic condition for which the values of these parameters were:

$$W = 0.465 \text{ lb} \quad \mu = 2.4$$

$$\frac{l}{b} = 4$$

$$\frac{x}{b} = 0.558$$

$$\frac{z}{b} = 0.225$$

$$\Gamma = 10^\circ \quad C_{z\beta} = -0.15$$

$$\frac{S_t}{S} = 7.5 \text{ percent} \quad C_{n\beta} = 0.06$$

A few tests were also made to determine the effect of varying the effective dihedral for zero-length towline. For these tests the model had three degrees of freedom about the tow attachment point. The values of the other parameters were the same as for the basic condition given above.

Test results are available only for towline lengths up to 4 spans because of the size of the tunnel test section. Analysis of the towline terms and calculations extending the range of towline length indicate that changing the length of the towline up to about 10 spans affects the lateral-stability characteristics appreciably, but further increase has only slight effect. Therefore, for towline lengths of 10 spans and greater, the trends which are found for the remaining parameters at the shorter towline length can be expected to prevail.

T H E O R E T I C A L C A L C U L A T I O N S

In addition to the experimental investigation an attempt was made to develop an approximate theoretical method for predicting the lateral-stability characteristics of the glider on a single towline. By use of this theoretical method, which is given in the appendix, calculations were made for various combinations of towline length, effective dihedral parameter $C_{z\beta}$, directional stability parameter $C_{n\beta}$, relative-density factor μ , and vertical and horizontal towline attachment position. A complete listing of the conditions for which the calculations were made is given in tables I and II. Inasmuch as the product of inertia was believed to be relatively unimportant for the low-relative-density condition of most of the model tests, the product-of-inertia factor k_{xz} , was assumed to be zero for most of the calculations.

The parameters used in the calculations were obtained either from tests or from calculations for the specific model condition. The source of each of these parameters is indicated in table I. Except in the relative-density derivatives, values of the derivatives for an angle of attack α of 2° and a towline angle ϵ of 25° were used in the calculations.

RESULTS AND DISCUSSION

The results of the investigation are presented in table II and in figures 6 and 7 in which lateral oscillations are presented in terms of the period and the reciprocal of the time to damp to one-half amplitude for each particular condition. The reciprocal of the time to damp to one-half amplitude is used to evaluate the damping because this value is a direct measure of the degree of stability. In general, the calculations and tests were made at the same conditions except where the dynamic characteristics of the model or physical limitations of the test setup precluded testing.

The lateral-stability characteristics determined by the theory presented in the appendix indicate that the lateral motions of the glider model generally consist of two highly damped aperiodic modes and two periodic modes, one usually having a period of approximately three times the other. From the results of the calculations and tests it appears that the long-period mode is usually the predominant or more lightly damped motion and consists of a combined rolling and yawing motion similar to that of the conventional Dutch roll.

Wherever possible the lateral-stability characteristics of both periodic modes were obtained from flight records similar to those of figure 5. In general, the characteristics of the predominant long-period mode were obtained from the plot of sidewise displacement against time (fig. 5(a)). The short-period mode appeared primarily as a yawing oscillation and its characteristics were obtained from plots of yaw angle against time (fig. 5(b)). In most cases it was difficult to ascertain the period and damping of the short-period oscillation because it was masked by the less heavily damped long-period oscillation.

Although no systematic investigation was conducted to determine the effect of towline angle on the lateral-stability characteristics of the glider model, analysis of the towline forces indicated its importance. Some exploratory tests were made to verify this analysis and it was found that, in general, for any attachment point in the range tested, increasing the towline angle was stabilizing. During the tests an attempt was made to hold the towline angle and angle of attack to one set of values ($\epsilon = 25^\circ$, $\alpha = 2^\circ$). Although these values of ϵ and α were not always exactly obtained, it is believed that the slight variations of these parameters do not invalidate the correlation of theoretical and test results.

CORRELATION OF CALCULATED AND EXPERIMENTAL RESULTS

The results of the experiments and analysis which are presented in table II and figures 6 and 7 indicate that, although the theory predicts the periods of the lateral oscillations fairly well, it does not predict the damping with sufficient accuracy to be of practical use.

In order to determine whether the omission of the product-of-inertia terms, recently found to be important in some cases (reference 4), was responsible for the poor quantitative agreement of the calculated and experimental damping results, additional calculations were made for the basic condition and for the relative-density-of-10 condition with these terms included in the equations. These calculations showed that inclusion of the product-of-inertia terms had virtually no effect on the results for the basic condition ($\mu = 2.4$) but did change appreciably the damping results of the higher relative-density condition ($\mu = 10.0$). Therefore, with the exception of the relative-density variation, product-of-inertia effects were ignored for these tests and calculations.

In view of the fact that only first-order effects were considered in developing the theory, the discrepancies between the theoretical and experimental results may in part be associated with the relative importance of some terms which were considered negligible to the first approximation.

Effect of $C_{\lambda\beta}$

Four-span towline length.- The experimental data for the range of $-C_{\lambda\beta}$ given in figure 6(a) show the periods of both the long-period and the short-period modes to be fairly constant. Although the short-period calculations are in good agreement with the tests, the long-period results indicate increasing length of period with decreasing effective dihedral.

The experimental damping results indicate that the long-period motion is the predominant mode since the short-period motion was always very heavily damped. The damping of the long-period oscillation was found to decrease with decrease in $-C_{\lambda\beta}$. At a value of $-C_{\lambda\beta}$ of -0.0458

(table II) any disturbance results in a rapid divergence in roll which obscures the characteristics of the oscillatory modes. The calculated results do not agree with the tests except in the prediction of the divergence.

Zero towline length.- The test results of figure 7 show that for the zero towline length the short-period oscillation is the predominant motion for all positive values of $-C_{\lambda\beta}$. The length of the period, however, increases as the value of $-C_{\lambda\beta}$ decreases indicating a

transition of the predominant motion from the short-period to a longer-period mode at low and negative effective dihedrals. The calculations show the short-period motion to be the predominant mode only at the higher values of $-C_{l\beta}$ and that the long period is the more lightly damped at

lower effective dihedrals. These results also clearly indicate that the long-period mode is replaced by a divergence as the value of $-C_{l\beta}$ is increased from 0 to -0.0458.

Effect of $C_{n\beta}$

The test results of figure 6(b) show little change in the period of the long-period oscillation for the range of $C_{n\beta}$ tested, whereas the period of the short-period oscillation increases gradually with reduction in $C_{n\beta}$. At zero directional stability the short-period motion which was hardly noticeable at higher values of $C_{n\beta}$ became evident as a steady large-amplitude short-period yawing oscillation. It was assumed that the motion was unstable at small amplitudes and built up to a steady oscillation of large amplitude. The rate of increase of amplitude could not be measured, however, because the oscillation was well developed by the time the trim conditions had been attained and the short-period yawing motion could not be stopped by the pilot to permit study of the motion at small amplitudes. The calculations show a marked decrease in the damping of the short-period mode with decrease in $C_{n\beta}$ and at $C_{n\beta} = 0$ indicate the unstable oscillation which was found experimentally.

With increase in the directional stability the damping of the long-period oscillation was found to increase slightly. The calculated results are not in agreement with this trend.

Effect of μ

An indication of the effect of the relative-density factor μ on the lateral-stability characteristics is given in figure 6(c). Because of test limitations imposed by the model, the angle of attack as well as airspeed had to be increased as the value of μ was increased. Table I gives the corresponding variation in the other parameters used for the calculations. Compared to the change in magnitude of the values of μ , the changes in the other parameters were relatively small, however, and the principal effect given in figure 6(c) is believed to be that of variation of μ .

Although the period of the long-period oscillation increases slightly with increase in relative density, the long-period calculated results show

a very slight decrease in length of the period. The inclusion of the product-of-inertia term in the calculations for a value of $\mu = 10$ had practically no effect on the period of either the long-period or the short-period oscillations. The experimental results show a general increase in damping of the long-period mode as the value of μ is increased from 2.4 to 10, but the calculated results presented in figure 6(c) indicated that increasing μ from an average present-day value of 2.4 to 10.0 results in a change from stability to gradually increasing instability for the long-period oscillation. Including the product-of-inertia terms in the calculations (table II) improves the agreement between damping results of the tests and calculations at a value of μ of 10 but produces virtually no change in the results at a value of μ of 2.4. Since the tests gave no indication of short-period instability at any value of relative density, it is apparent that including the product-of-inertia terms in the calculations made the agreement between the tests and calculations poorer for the short-period mode.

Effect of Tow Attachment Point

The effect of varying the horizontal location of the tow attachment point was not determined experimentally because the model could not be trimmed longitudinally for values of x below that of the basic condition. However, calculations were made for a range of values of x from 0 to 0.558 spans, and these results are presented in figure 6(d) with the one experimental point available. The results show a decrease in the instability of the long-period motion and a decrease in damping of the short-period motion with increase in x . With increase in x , the period of the long-period oscillation decreases at a decreasing rate and the length of the short-period oscillation is practically constant. The effect of the vertical location of the tow attachment point is given in figure 6(e). Increasing the z distance was found to have little effect on the length of the period of either mode but reduced the length of the longer-period mode slightly. The test results show that the greatest damping was found at a value of z of 0.117 and that increasing or decreasing the horizontal distance reduced the damping of the long-period mode. The calculations indicate, however, that increasing z improves the stability of the long-period mode but reduces the short-period damping.

Effect of Towline Length

Both the theoretical and experimental results presented in figure 6(f) indicate that increasing the towline length from 1 to 4 span lengths increases the damping of the long-period oscillation. The test results, however, show somewhat more damping than is predicted by the theory. Calculations were also made for towline lengths of 10 and 100 spans although tests were not possible for these lengths. The long-period damping continues to increase (table II) but at a much more gradual rate than was found for the range tested.

The calculated results show that increasing the towline length from .1 to 100 span lengths has no appreciable effect on the damping of the short-period oscillation.

An increase in the towline length causes a gradual increase in the period of the long-period oscillation but causes no change in the period of the short-period oscillation. These results are shown by both the calculated and experimental results which are in good agreement.

C O N C L U D I N G R E M A R K S

The results of the experimental investigation and theoretical analysis to determine the lateral-stability characteristics of a glider towed by a single towline may be summarized as follows:

1. The investigation showed that it is possible to obtain inherent lateral stability with a single-towline-glider arrangement.

2. The stability theory presented in the present paper does not predict the stability of the glider model with sufficient accuracy to be of much practical value. The calculated and experimental results are in fairly good agreement on the period of the lateral oscillations and the prediction of divergences, but the calculated damping of the lateral oscillation is generally considerably less than the measured damping. The theory is presented, however, as a basis for further study and the experimental results should be useful for correlation with any further theoretical work which may be performed.

Langley Aeronautical Laboratory
National Advisory Committee for Aeronautics
Langley Field, Va.

A P P E N D I X

THEORETICAL METHOD

The method of calculating the lateral stability of a glider towed by a single towline consisted of setting up the stability equations with respect to the stability axes of the glider (see fig. 1), obtaining the aerodynamic stability derivatives for the glider and the derivatives caused by the towline forces, and solving for the period and time to damp of the lateral oscillatory modes of the glider.

Assumptions.- To simplify and facilitate the handling of the theoretical analysis, the following assumptions were made:

1. The glider and tug were assumed to be in level flight and the tug to be in steady flight.
2. The basic aerodynamic parameters were assumed to vary independently of each other.
3. Lateral-stability characteristics were assumed to be independent of the longitudinal-stability characteristics.
4. The angles of deviation of the glider from the steady-flight condition were assumed to be small. Towline angles with respect to the relative wind and towline tension were assumed not to change during a disturbance.
5. The towline was assumed to be weightless and straight and to have no effect on the stability of the glider other than that caused by direct forces and moments resulting from towline tension.

Full-scale tests and tests in the Langley free-flight tunnel have indicated that the assumption of a straight towline is valid for moderate towline lengths. British investigations show that glider towlines can be considered straight for lengths up to about 4 or 5 spans for any towline angle and for greater lengths for towline angles between about 20° to 30°.

Equations of motion.- Inasmuch as a single towline allows the glider three degrees of lateral freedom, the basic lateral-stability equations were used, modified only to include the derivatives defining towline restraints. The lateral equations of motion following a disturbance may be written as follows:

$$m \frac{dV}{dt} + mVr = mg\phi + \beta Y\beta + \text{towline derivatives} \quad (1)$$

$$mk_Z^2 \frac{dr}{dt} = mk_{XZ} \frac{dp}{dt} + \frac{pb}{2V} N_p + \frac{rb}{2V} N_r + \beta N\beta + \text{towline derivatives} \quad (2)$$

$$mk_X^2 \frac{dp}{dt} = \frac{pb_L}{2V^2 p} + mk_{XZ} \frac{dr}{dt} + \frac{rb_L}{2V^2 r} + \beta L_\beta + \text{towline derivatives} \quad (3)$$

If the effect of glide-path angles other than zero is considered, the normal glide-path terms will appear in the basic lateral-stability portion of the preceding equations.

Towline derivatives.- In straight steady flight the towline contributes only a pitching moment and does not affect the lateral stability. Sidewise displacement of the glider along the Y-axis, displacements in yaw about the Z-axis, or displacements in roll about the X-axis result in forces and moments about these axes that are functions of towline tension. The towline derivatives expressing the resultant relationship may be obtained to the first order as follows from figure 8 by consideration of the forces and moments with respect to the stability axes and the glider center of gravity:

(a) Lateral-force derivatives

$$\frac{Y}{T} = -\frac{Y}{l}$$

or

$$Y_Y = -\frac{T}{l} \quad (4)$$

and

$$\frac{Y}{T} = -\frac{x \sin \psi}{l} - (\cos \epsilon \sin \psi')$$

but for relatively long towlines, however, $\psi' = \psi$ then

$$Y_\psi = -T \left(\frac{x}{l} + \cos \epsilon \right) \quad (5)$$

where $\sin \psi' = \psi$ and

$$\frac{Y}{T} = -\frac{z}{l} \sin \phi - \sin \epsilon \sin \phi$$

Also for long towlines, $\phi' = \phi$ or

$$Y_\phi = -T \left(\frac{z}{l} + \sin \epsilon \right) \quad (6)$$

where $\sin \phi = \phi$.

(b) Yawing-moment derivatives:

$$N_Y = -\frac{Tx}{l} \quad (7)$$

$$N_{\psi} = -Tx \left(\frac{x}{l} + \cos \epsilon \right) \quad (8)$$

$$N_{\phi} = -Tx \left(\frac{z}{l} + \sin \epsilon \right) \quad (9)$$

(c) Rolling-moment derivatives:

$$L_y = -\frac{Tz}{l} \quad (10)$$

$$L_{\psi} = -Tz \left(\frac{x}{l} + \cos \epsilon \right) \quad (11)$$

$$L_{\phi} = -Tz \left(\frac{z}{l} + \sin \epsilon \right) \quad (12)$$

where $T = -\frac{\text{Drag}}{\cos \epsilon}$ and

$$\epsilon = \tan^{-1} \left(\frac{W - L}{D} \right)$$

For zero towline length, the tow attachment point is fixed relative to the tug and the towline tension always acts in the vertical plane of the relative wind. Because of these limitations the glider is permitted only three degrees of freedom and the towline derivatives Y_y , N_y , and L_y normally resulting from sidewise displacement of the tow attachment point do not exist. The remaining derivatives resulting from yaw and roll about the tow attachment point become:

(a) Lateral-force derivatives:

$$Y_{\psi} = -T \cos \epsilon \quad (5a)$$

$$Y_{\phi} = -T \sin \epsilon \quad (6a)$$

(b) Yawing-moment derivatives:

$$N_{\psi} = -Tx \cos \epsilon \quad (8a)$$

$$N_{\phi} = -Tx \sin \epsilon \quad (9a)$$

(c) Rolling-moment derivatives:

$$L_{\psi} = -Tz \cos \epsilon \quad (11a)$$

$$L_{\phi} = -Tz \sin \epsilon \quad (12a)$$

Equations of motion, nondimensional form.- Substituting the towline derivatives in equations (1), (2), and (3) yields the following equations:

$$m \frac{dv}{dt} + mVr - mg\phi - \beta Y_\beta - \gamma Y_\gamma - \psi Y_\psi - \phi Y_\phi = 0 \quad (13)$$

$$mk_X^2 \frac{dr}{dt} - mk_{XZ} \frac{dp}{dt} - \frac{pb}{2V} N_p - \frac{rb}{2V} N_r - \beta N_\beta - \gamma N_\gamma - \psi N_\psi - \phi N_\phi = 0 \quad (14)$$

$$mk_X^2 \frac{dp}{dt} - \frac{pb}{2V} L_p - mk_{XZ} \frac{dr}{dt} - \frac{rb}{2V} L_r - \beta L_\beta - \gamma L_\gamma - \psi L_\psi - \phi L_\phi = 0 \quad (15)$$

For convenience, the equations can be converted to nondimensional form by using the following relationships and the operator D:

$$y' = \frac{y}{b}$$

$$\mu = \frac{m}{\rho S b}$$

$$K_x = \frac{k_x}{b}$$

$$K_z = \frac{k_z}{b}$$

$$y = V \int (\beta + \psi) dt = \left(\frac{\beta + \psi}{D} \right) b$$

$$\frac{dy}{dt} = v$$

$$\frac{d\phi}{dt} = p$$

$$\frac{d\psi}{dt} = r$$

$$\frac{v}{V} = \beta$$

$$D = \frac{d}{ds}$$

where

$$s = \frac{Vt}{b}$$

and

$$ds = \frac{V}{b} dt$$

$$\frac{D\phi}{2} = \frac{pb}{2V}$$

$$\frac{D\psi}{2} = \frac{rb}{2V}$$

Then substituting these relationships and dividing equation (13) by $\frac{\rho}{2}SV^2b$ yields the nondimensional equations:

$$\begin{aligned} & \left(2\mu D^3 - C_{Y\beta} D^2 - T_{y_y', D} \right) \beta + \left(4\mu D^2 - 2T_{y_\psi} D - 2T_{y_y'} \right) \frac{rb}{2V} \\ & + \left(-2C_{wD} - 2T_{y\phi} D \right) \frac{pb}{2V} = 0 \end{aligned} \quad (16)$$

$$\begin{aligned} & \left(-C_{n\beta} D^2 - T_{n_y', D} \right) \beta + \left(4\mu K_Z^2 D^3 - C_{n_r} D^2 - 2T_{n_\psi} D - 2T_{n_y'} \right) \frac{rb}{2V} \\ & + \left(-4\mu K_{XZ} D^3 - C_{n_p} D^2 - 2T_{n\phi} D \right) \frac{pb}{2V} = 0 \end{aligned} \quad (17)$$

$$\begin{aligned} & \left(-C_{l\beta} D^2 - T_{l_y', D} \right) \beta + \left(-4\mu K_{XZ} D^3 - C_{l_r} D^2 - 2T_{l_\psi} D - 2T_{l_y'} \right) \frac{rb}{2V} \\ & + \left(4\mu K_X^2 D^3 - C_{l_p} D^2 - 2T_{l\phi} D \right) \frac{pb}{2V} = 0 \end{aligned} \quad (18)$$

where the nondimensional forms of the towline derivatives are:

$$T_{y_y'} = -\frac{C_T}{l}; \quad C_T \text{ being } \frac{C_D}{\cos \epsilon}$$

$$T_{y_\psi} = -C_T \left(\frac{x}{l} + \cos \epsilon \right)$$

$$T_{y\phi} = -C_T \left(\frac{z}{l} + \sin \epsilon \right)$$

$$T_{n_y'} = -xT_{y_y'}$$

$$T_{n_\psi} = -xT_{y_\psi}$$

$$T_{n_\phi} = -xT_{y_\phi}$$

$$T_{l_y} = -zT_{y_y'}$$

$$T_{l_\psi} = -zT_{y_\psi}$$

$$T_{l_\phi} = -zT_{y_\phi}$$

The determinant of the left side of these equations yields the glider-stability equation of the form:

$$AD^9 + BD^8 + CD^7 + ED^6 + FD^5 + GD^4 + HD^3 + ID^2 + JD + K = 0 \quad (19)$$

where:

$$A = 32\mu^3 K_Z^2 K_X^2 - 32\mu^3 K_{XZ}^2$$

$$B = -8\mu^2 K_Z^2 C_{l_p} - 16\mu^2 K_X^2 K_Z^2 C_{Y_\beta} - 8\mu^2 K_{XZ} C_{n_p} + 16\mu^2 K_{XZ}^2 C_{Y_\beta} \\ - 8\mu^2 K_{XZ}^2 C_{l_r} - 8\mu^2 K_X^2 C_{n_r}$$

$$C = -16\mu^2 K_Z^2 T_{l_\phi} - 16\mu^2 K_X^2 T_{n_\psi} - 16\mu^2 K_X^2 K_Z^2 T_{y_y'} + 2\mu C_{n_r} C_{l_p} \\ - 2\mu C_{n_p} C_{l_r} + 4\mu K_Z^2 C_{Y_\beta} C_{l_p} + 4\mu K_X^2 C_{Y_\beta} C_{n_r} + 16\mu^2 K_X^2 C_{n_p} + 16\mu^2 K_{XZ}^2 C_{l_\beta} \\ - 16\mu^2 K_{XZ} T_{n_\phi} + 4\mu K_{XZ} C_{n_p} C_{Y_\beta} + 16\mu^2 K_{XZ}^2 T_{y_y'} + 4\mu K_{XZ} C_{Y_\beta} C_{l_r} - 16\mu^2 K_{XZ} T_{l_\psi}$$

$$\begin{aligned}
 E = & 4\mu C_{n_r} T_{l\phi} + 4\mu C_{l_p} T_{n\psi} - 4\mu C_{n_p} T_{l\psi} - 4\mu C_{l_r} T_{n\phi} + 8\mu K_Z^2 C_{Y\beta} T_{l\phi} \\
 & + 8\mu K_X^2 C_{Y\beta} T_{n\psi} + 4\mu K_Z^2 C_{l_p} T_{y'y'} + 4\mu K_X^2 C_{n_r} T_{y'y'} - 8\mu K_X^2 C_{n\beta} T_{y\psi} \\
 & - 8\mu K_Z^2 C_{l\beta} T_{y\phi} - C_{Y\beta} C_{n_r} C_{l_p} + C_{Y\beta} C_{n_p} C_{l_r} - 4\mu C_{n\beta} C_{l_p} + 4\mu C_{l\beta} C_{n_p} \\
 & - 8\mu K_Z^2 C_{l\beta} C_W - 8\mu K_{XZ} T_{y\psi} C_{l\beta} - 8\mu K_{XZ} C_W C_{n\beta} - 8\mu K_{XZ} T_{y\phi} C_{n\beta} \\
 & + 8\mu K_{XZ} T_{n\phi} C_{Y\beta} + 4\mu K_{XZ} T_{y'y'} C_{l_r} + 8\mu K_{XZ} C_{Y\beta} T_{l\psi} + 4\mu K_{XZ} C_{n_p} T_{y'y'}
 \end{aligned}$$

$$\begin{aligned}
 F = & -2C_{Y\beta} C_{n_r} T_{l\phi} + 2C_{Y\beta} C_{n_p} T_{l\psi} - 2C_{Y\beta} C_{l_p} T_{n\psi} + 2C_{Y\beta} C_{l_r} T_{n\phi} \\
 & - C_{n_r} C_{l_p} T_{y'y'} + C_{n_p} C_{l_r} T_{y'y'} - 8\mu C_{n\beta} T_{l\phi} + 8\mu C_{l\beta} T_{n\phi} + 2C_{n\beta} C_{l_p} T_{y\psi} \\
 & - 2C_{n\beta} C_{l_r} T_{y\phi} + 2C_{l\beta} C_{n_r} T_{y\phi} - 2C_{l\beta} C_{n_p} T_{y\psi} + 8\mu K_X^2 C_{Y\beta} T_{n\psi} \\
 & - 8\mu K_X^2 C_{n\beta} T_{y'y'} - 8\mu K_{XZ} T_{y'y'} C_{l\beta} - 8\mu K_{XZ} C_W T_{n\psi} + 8\mu K_{XZ} C_{Y\beta} T_{l\psi} \\
 & - 8\mu K_Z^2 C_W T_{l\psi} + 2C_{l\beta} C_{n_r} C_W - 2C_{n\beta} C_{l_r} C_W
 \end{aligned}$$

$$\begin{aligned}
 G = & 4C_{l\beta} C_W T_{n\psi} - 4C_{n\beta} C_W T_{l\psi} + 2C_{n_r} C_W T_{l\psi} - 2C_{l_r} C_W T_{n\psi} - 2C_{Y\beta} C_{l_p} T_{n\psi} \\
 & + 2C_{Y\beta} C_{n_p} T_{l\psi} + 2C_{n\beta} C_{l_p} T_{y'y'} - 2C_{l\beta} C_{n_p} T_{y'y'}
 \end{aligned}$$

$$H = -4C_{n\beta} C_W T_{l\psi} + 4T_{n\psi} C_{l\beta} C_W$$

$$I = J = K = 0$$

The period and time to damp to one-half amplitude of the oscillatory and aperiodic modes may be determined from the roots of equation 19 by the following relationships

$$P = \frac{2\pi}{d} \frac{b}{V}$$

$$\frac{T_1}{2} = -\frac{\log_e 0.5}{c} \frac{b}{V}$$

or

$$\frac{T_1}{2} = -\frac{0.0693}{c} \frac{b}{V}$$

where d is the coefficient of the imaginary portion of the complex roots and c is either the real portion of the complex roots for the oscillatory mode or the real root defining the aperiodic modes.

R E F E R E N C E S

1. Pitkin, Marvin, and McKinney, Marion O., Jr.: Flight Tests of a Glider Model Towed by Twin Parallel Towlines. NACA RB No. 3D30, 1943.
2. Pitkin, Marvin, and McKinney, Marion O., Jr.: Theoretical Analysis of the Lateral Stability of a Glider Towed by Twin Parallel Towlines. NACA ARR No. 3K17, 1943.
3. Shortal, Joseph A., and Osterhout, Clayton J.: Preliminary Stability and Control Tests in the NACA Free-Flight Wind Tunnel and Correlation with Full-Scale Flight Tests. NACA TN No. 810, 1941.
4. Sternfield, Leonard: Effect of Product of Inertia on Lateral Stability. NACA TN No. 1193, 1947.
5. Pearson, Henry A., and Jones, Robert T.: Theoretical Stability and Control Characteristics of Wings with Various Amounts of Taper and Twist. NACA Rep. No. 635, 1938.

TABLE I.- PHYSICAL AND AERODYNAMIC CHARACTERISTICS
OF THE SINGLE TOWLINE GLIDER MODEL

Wing area, square feet	1.02
Wing span, feet	2.50
Wing aspect ratio	6.10
Wing mean aerodynamic chord, feet	0.416
Model center-of-gravity location, percent mean chord	0.390

Mass characteristics (All values obtained by measurement)						
Weight W	Relative-density factor	k_X	k_{X_p}	k_Z	k_{Z_p}	k_{YZ}
^a 211	2.4	0.419	0.462	0.606	0.596	-0.0240
450	5.0	.364	-----	.543	-----	-----
720	8.0	.289	-----	.431	-----	-----
900	10.0	.259	.259	.388	.388	-.0143

Aerodynamic characteristics						
μ	α_o (deg)	C_L (b)	C_D (b)	C_{L_r} (c)	C_{n_p} (c)	C_{l_p} (c)
^a 2.4	10	0.57	0.110	0.161	-0.0272	-0.49
5.0	12	.75	.150	.221	-.0374	-.49
8.0	14	.86	.168	.282	-.0476	-.49
10.0	15	.92	.175	.322	-.0544	-.49

Vertical tail	Area (percent S)	C_{n_β} (b)	C_{y_β} (b)	C_{nr} (b)
	0	0	-0.2574	-0.020
^a 1	5.0	.0343	-.4061	-.040
^a 2	7.5	.0572	-.4462	-.060
3	10.0	.1087	-.5205	-.082

Dihedral angle (deg)	C_{l_β} (b)
-5	0.0458
0	0
5	-.0688
^c 10	-.1375
15	-.2000

^aBasic condition from which the parameters were varied.

^bValues obtained from force tests in the Langley free-flight tunnel.

^cValues obtained from reference 5.

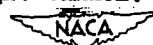


TABLE II.- CORRELATION OF THE THEORETICAL AND EXPERIMENTAL RESULTS OF THE LATERAL STABILITY INVESTIGATION OF A GLIDER TOWED BY A SINGLE TOWLINE

Variable	Conditions							Theory						Tests										
	Γ (deg)	Vertical tail (percent B)	μ	x	z	l	Airspeed (fps)	Aperiodic mode		Oscillatory mode				Aperiodic mode	Oscillatory mode				α (deg)	α (deg)				
								$\frac{1}{T_1}$	P	Long period		Short period			P	$\frac{1}{T_1}$	P	$\frac{1}{T_1}$			Long period		Short period	
										$\frac{1}{T_1}$	P	$\frac{1}{T_1}$	P								P	$\frac{1}{T_1}$	P	$\frac{1}{T_1}$
C _{1β}	-5 0 5 10 15	7.5	2.4	0.558	0.225	4	24.8	25.8 25.9 26.2 26.3 26.4	-0.93 .96	4.67 3.96	0.622 -.014	0.92 .92	1.667 1.337	(d)	3.85 3.90 2.60 3.75	0.07 .35 .16 .45	0.80 1.00 .95 1.00	26 26 24 26	1 1 1/2 2 3					
																				-5 0 5 10	7.5	2.4	.558	.225
C _{2β}	10	0.0 5.0 10.0	2.4	.558	.225	4	24.8	26.3 26.3 26.3 26.3	2.71 2.76 2.45 2.34	2.33 2.34 2.63 1.96	.217 .075 .011 -.0001	1.16 .97 .39	-.922 -.190 .331 .835	2.60 2.60 2.60	.21 .16 .34	1.35 1.35 1.35	(d)	26 25 25	2 2 2					
																				μ	10	7.5	2.4	.558
z	10	7.5	2.4	.186 .372 .558	.225	4	24.8	26.3 26.3 26.3	1.53 2.08 2.36 2.45	4.13 3.12 2.76 2.63	-.471 -.357 -.179 .011	1.18 1.07 .98 .89	1.300 .916 .964 .331	No tests No tests No tests 2.60	.17 .42 .16	.65 .60 .95	24 24 26	2 2 1 1/2						
																			x	10	7.5	2.4	.558	.033 .117 .225
l	10	7.5	2.4	.558	.225	1 1.7 2 3 4 10 100	24.8	26.0 26.2 26.3 26.3 26.4 26.4	3.87 3.19 2.77 2.45 1.49 3.66	1.82 2.19 2.41 2.63 3.25 3.66	-.460 .87 .88 .89 .409 .91	.86 .370 .389 .331 .366 .891	2.00 2.60 2.90 2.60	.37 (a) .10 .16	.65 .60 .95	25 25 21 24	2 2 1 2							

aConditions for all calculations: α = 2°, ε = 25°.
 bBasic condition from which the parameters were varied.
 cIncluding product-of-inertia terms.
 dUnstable - from visual observation.
 eNeutrally stable from visual observation.



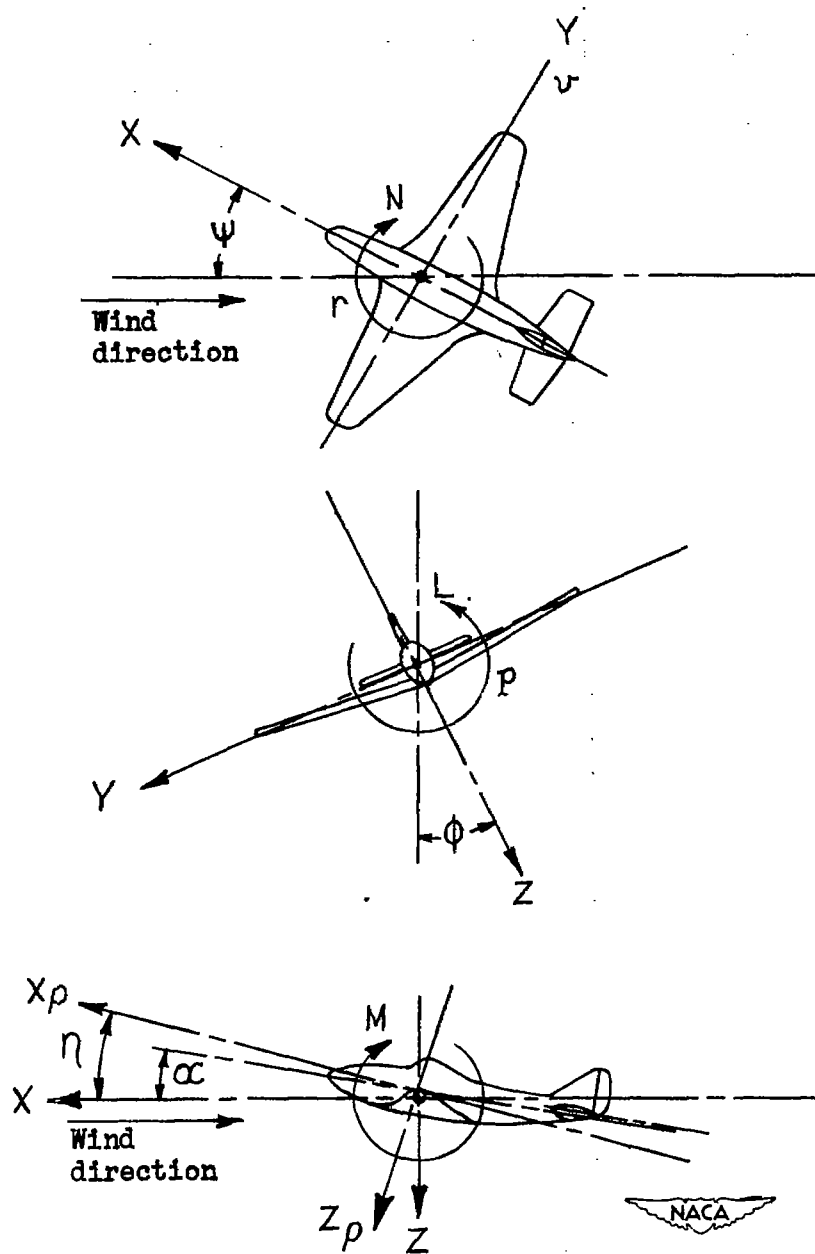
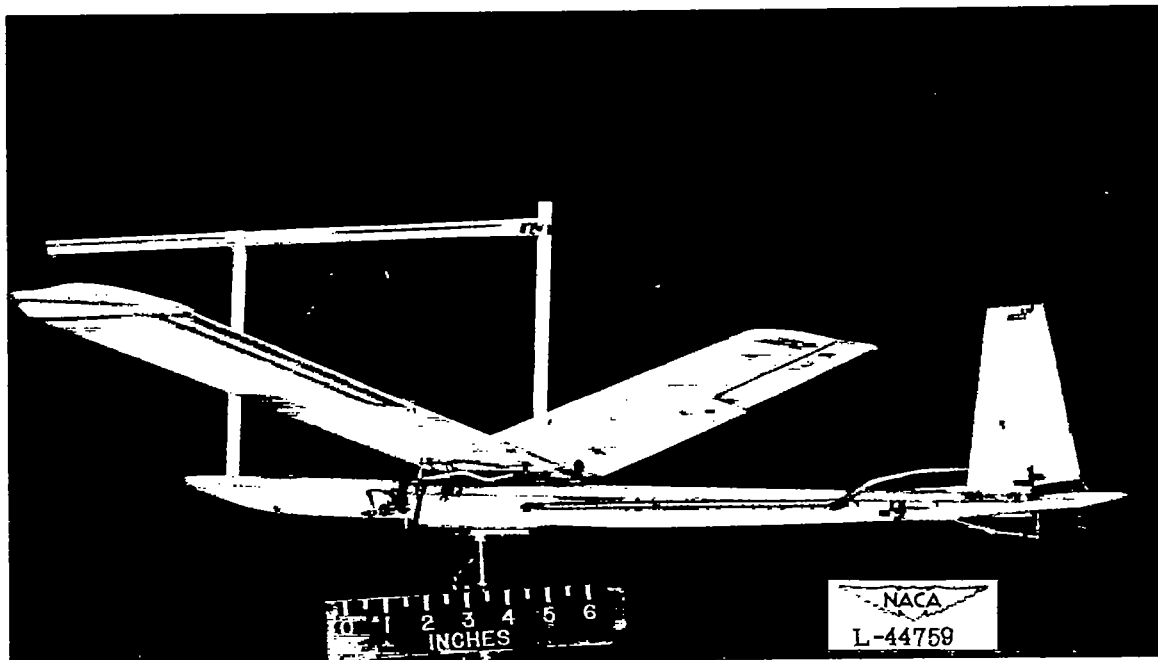
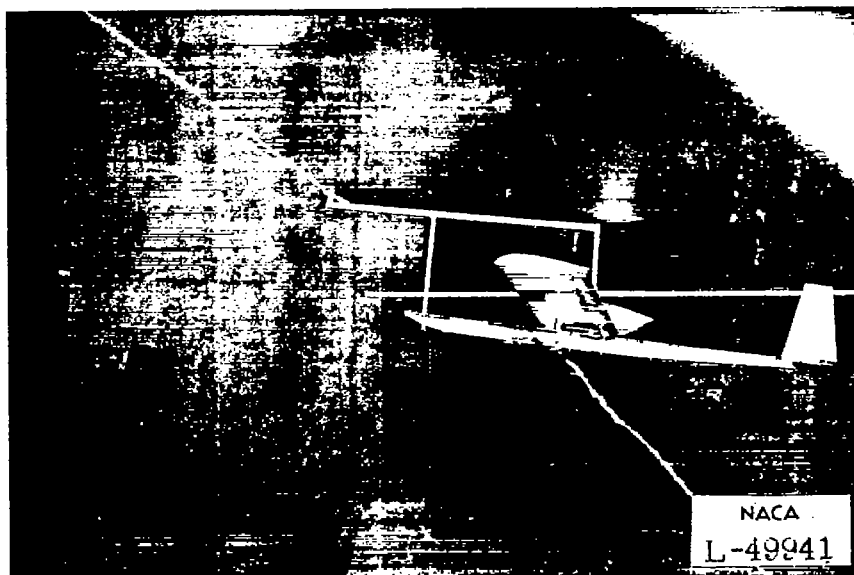


Figure 1.- The stability system of axes. Arrows indicate positive directions of moments, forces, and velocities.

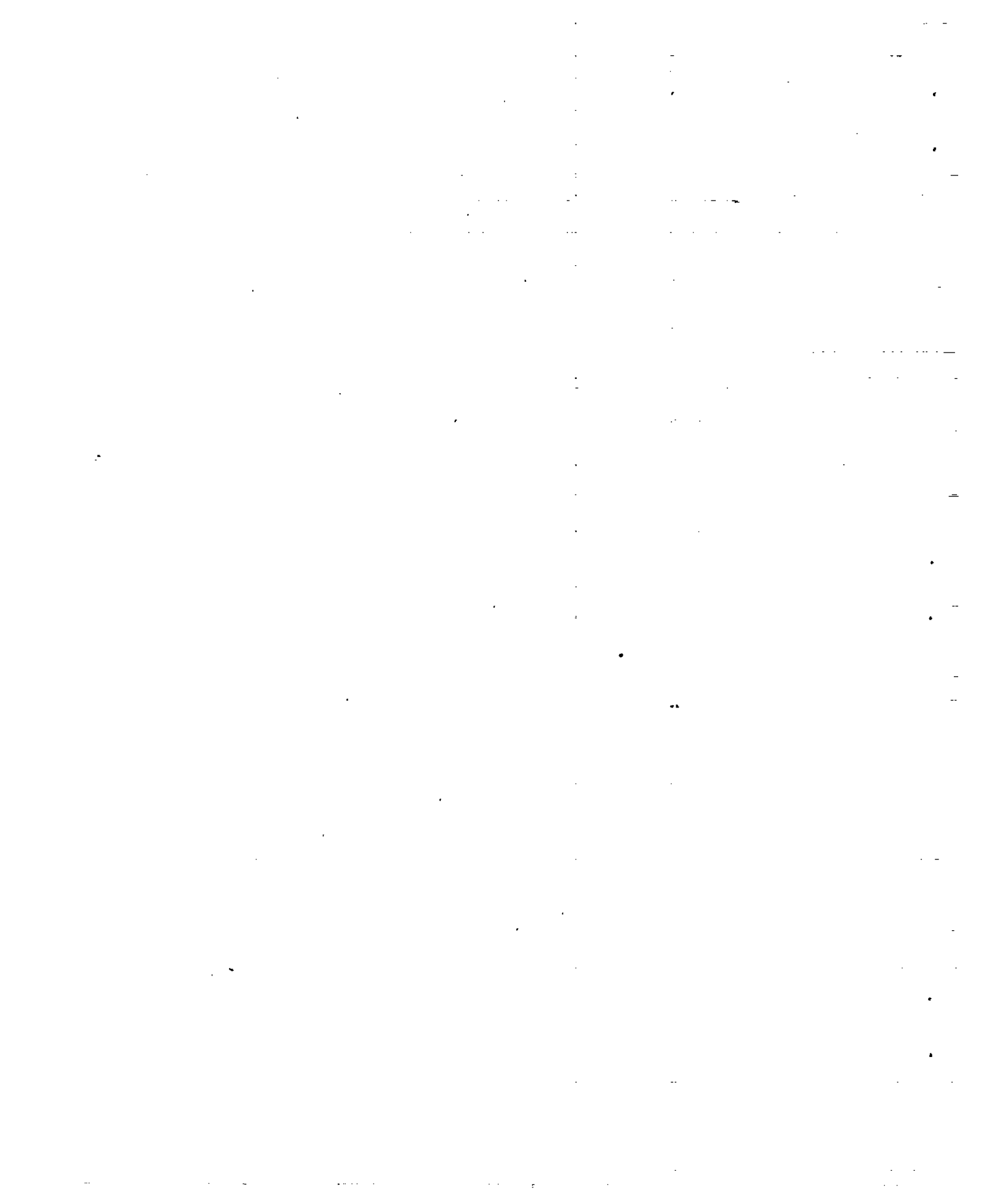


(a) Mounted on a stand.



(b) In flight.

Figure 2.- The glider model used in the tow tests.



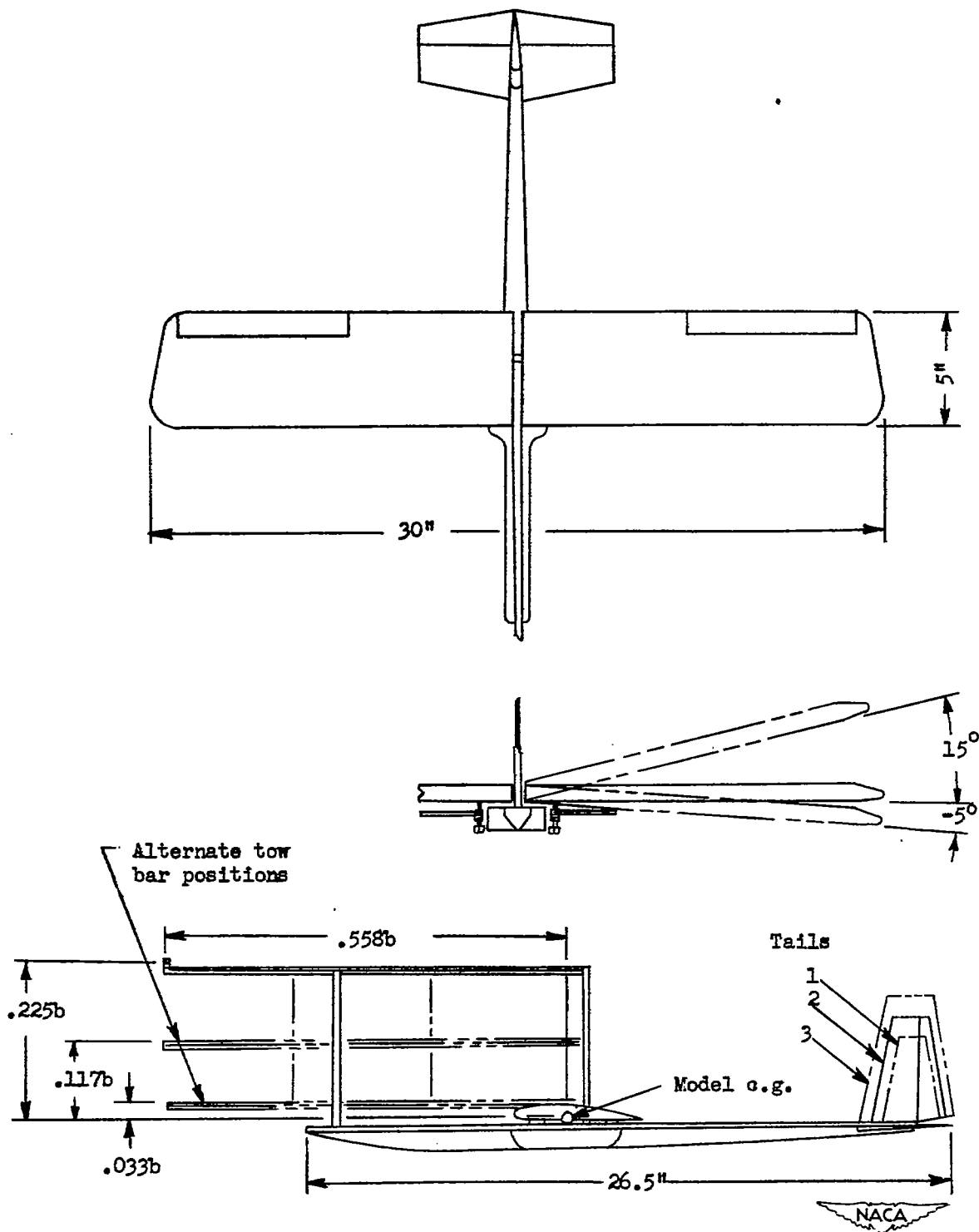


Figure 3.- Sketch of the glider model.

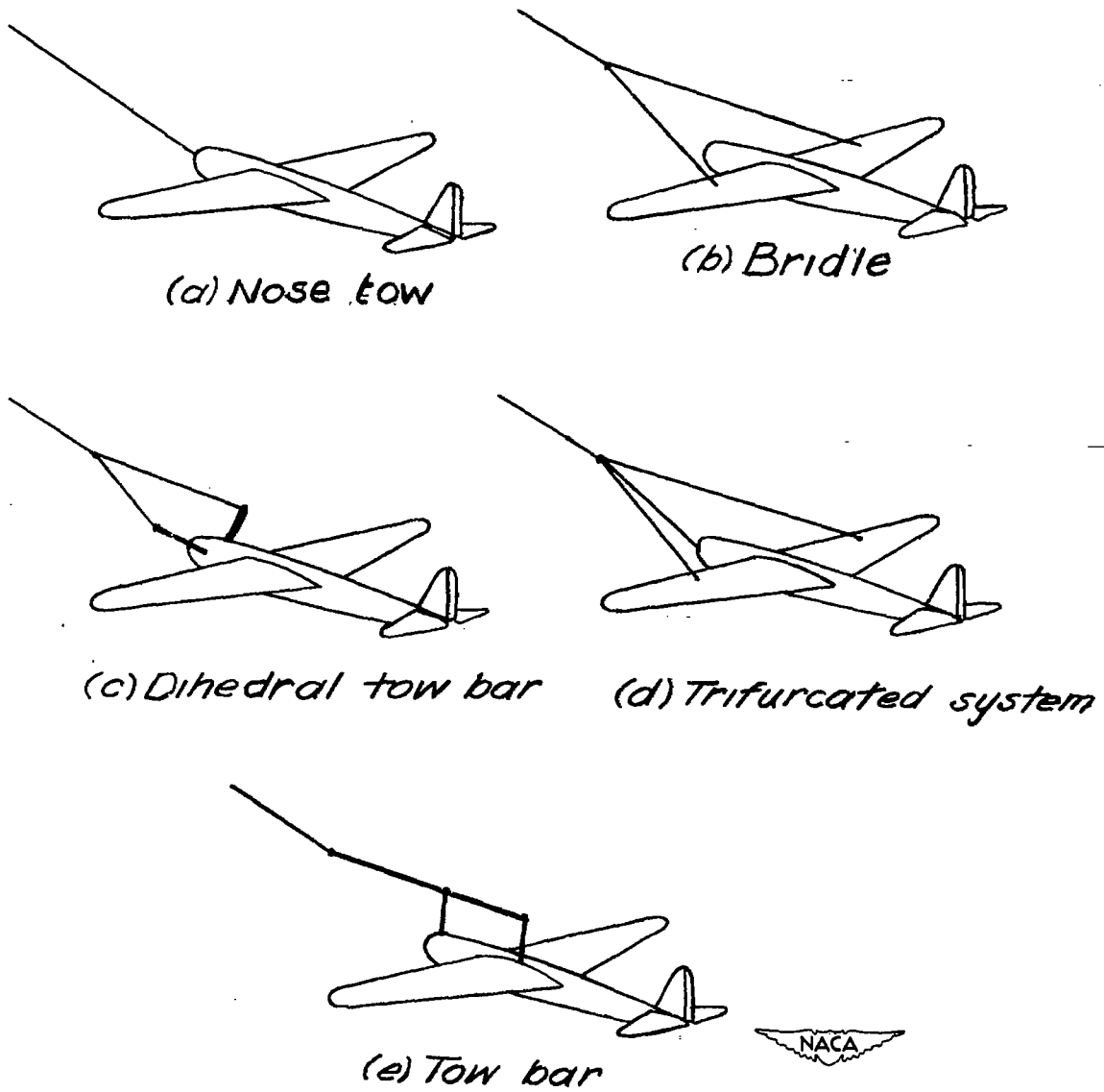
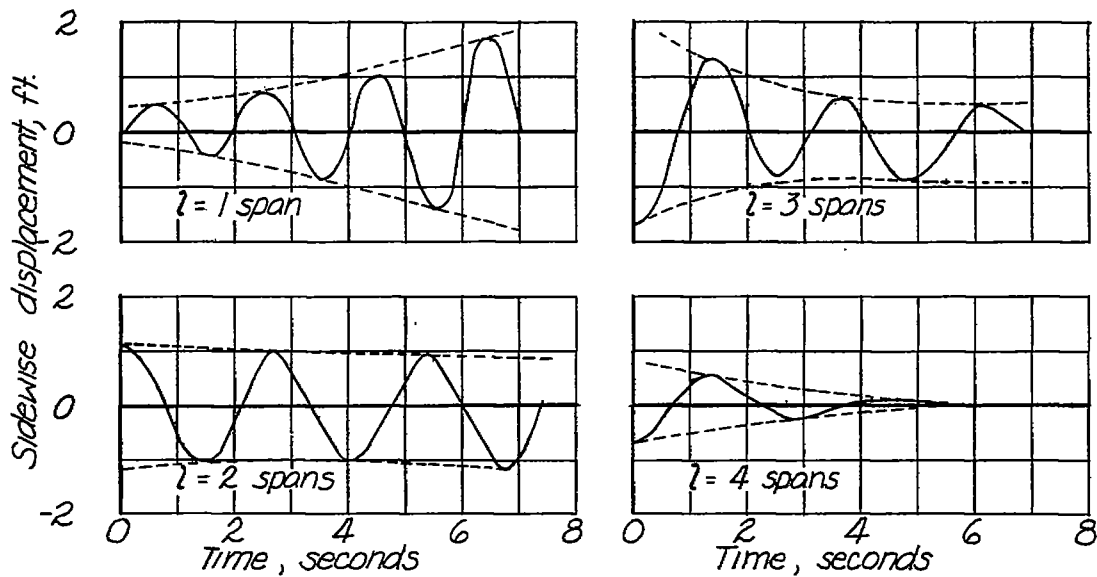
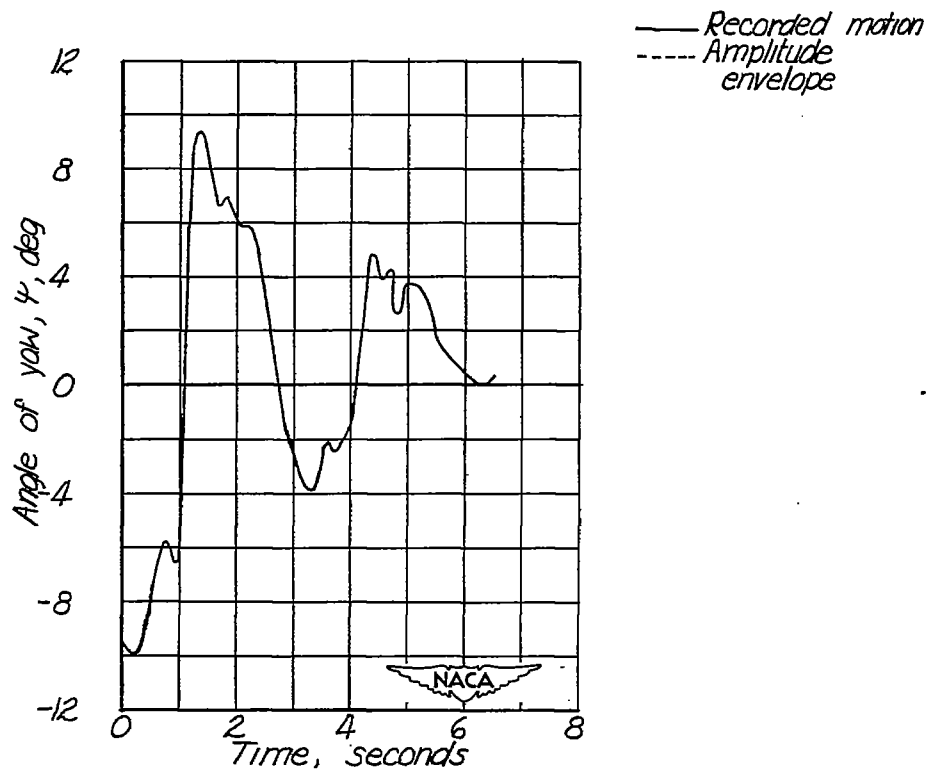


Figure 4.- Glider tow systems employing a single towline.



(a) Sidewise displacement.



(b) Yaw angle.

Figure 5.- Typical records of lateral motions as obtained from motion-picture records of tow tests of the glider model.

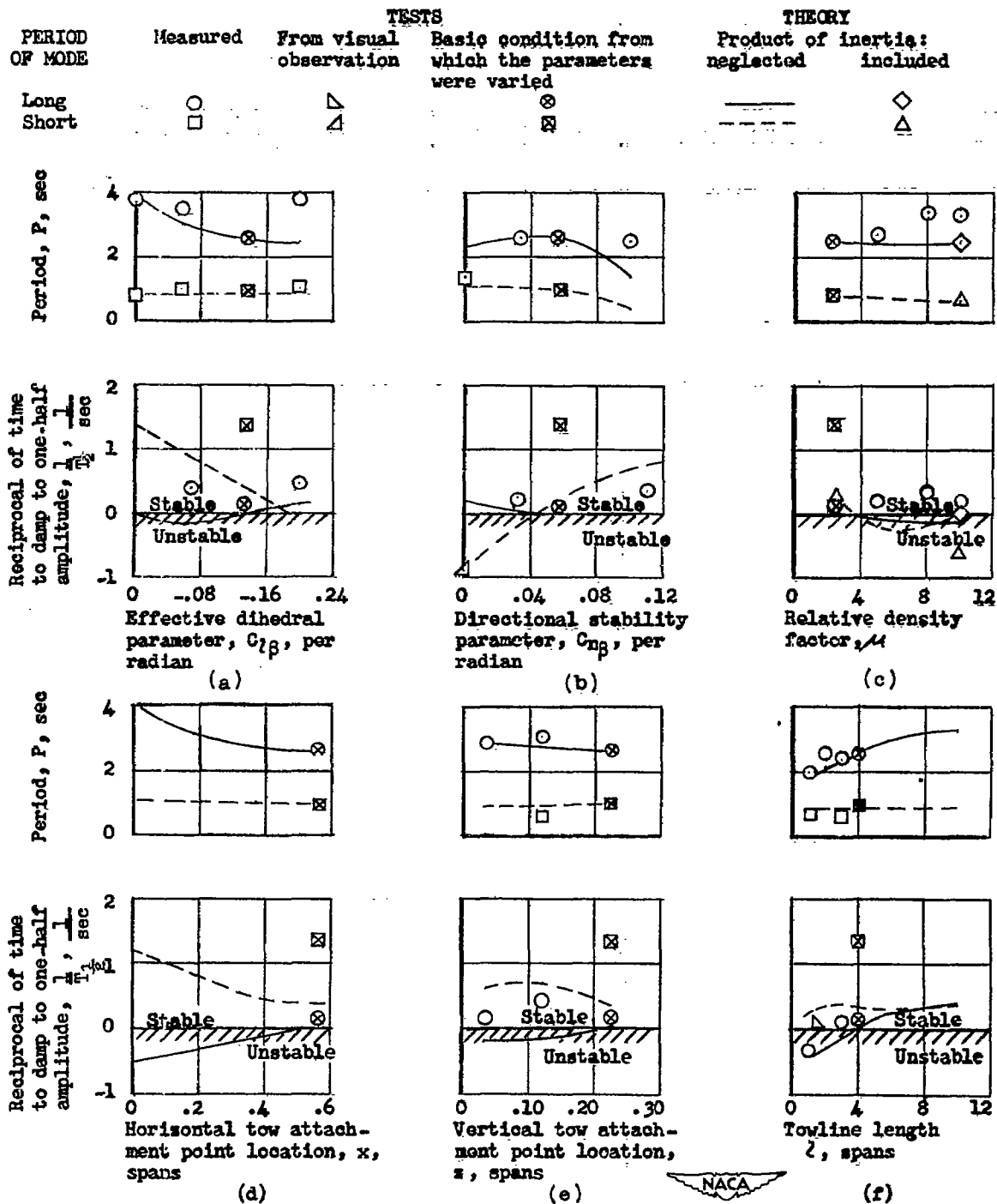


Figure 6.- Correlation of the period and the reciprocal of the time to damp to one-half amplitude of the lateral oscillations of the glider model as obtained from tests and theory. (See table II for complete conditions of each part.)



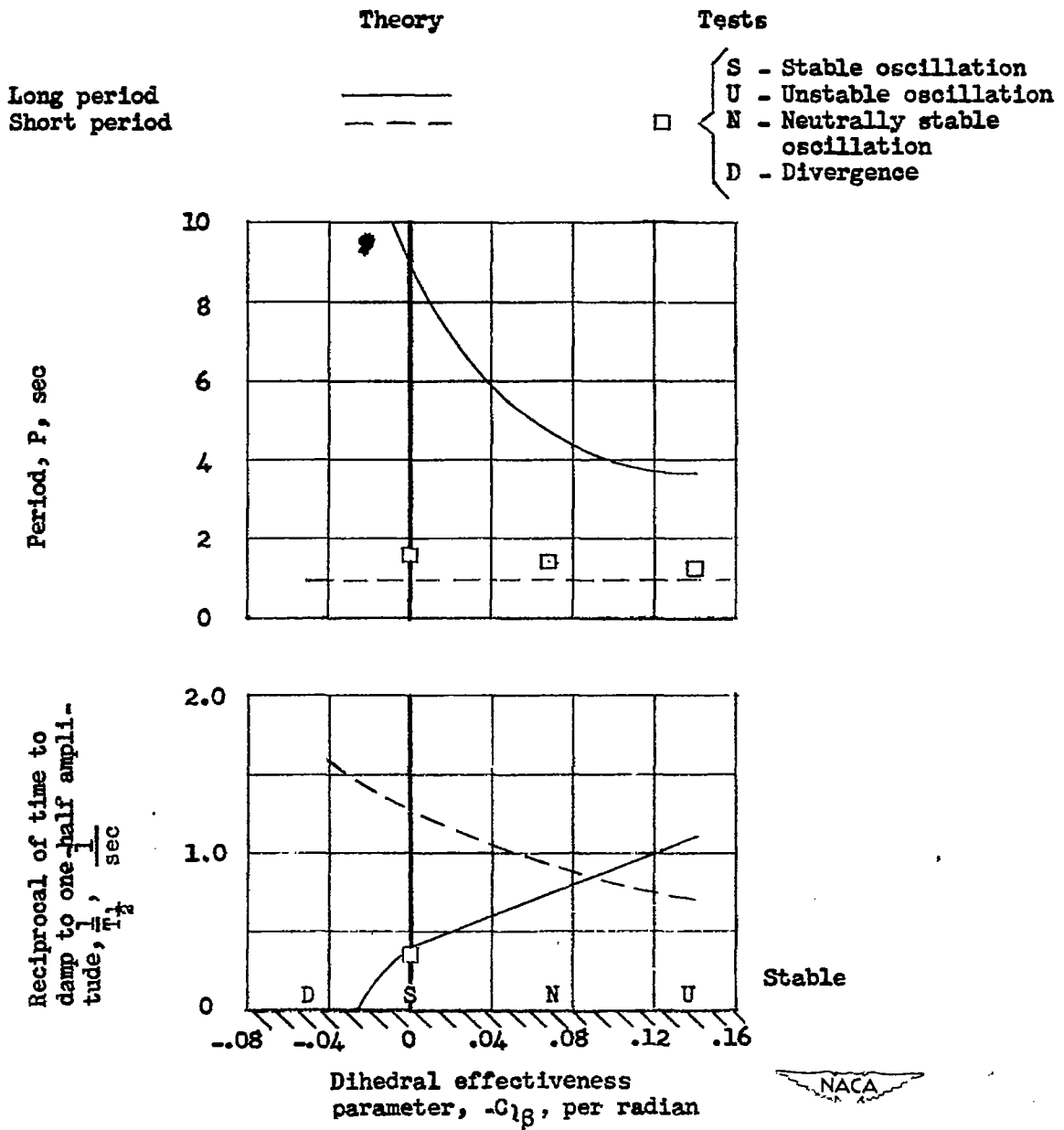
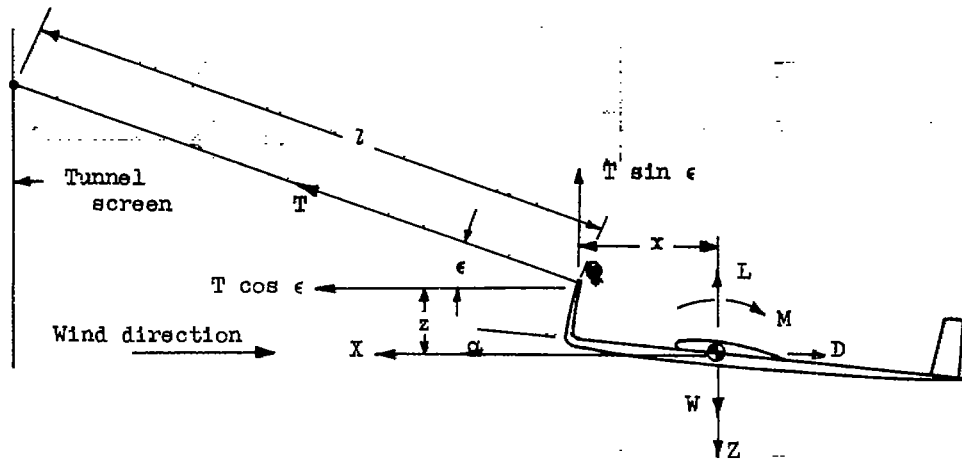
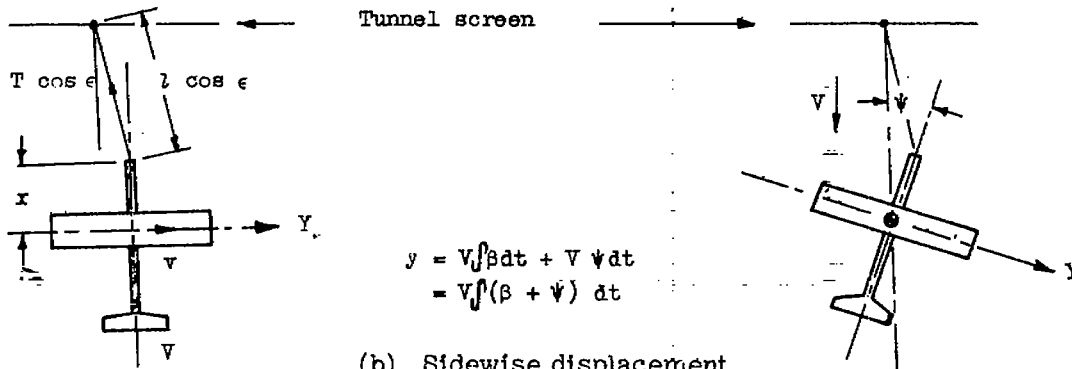


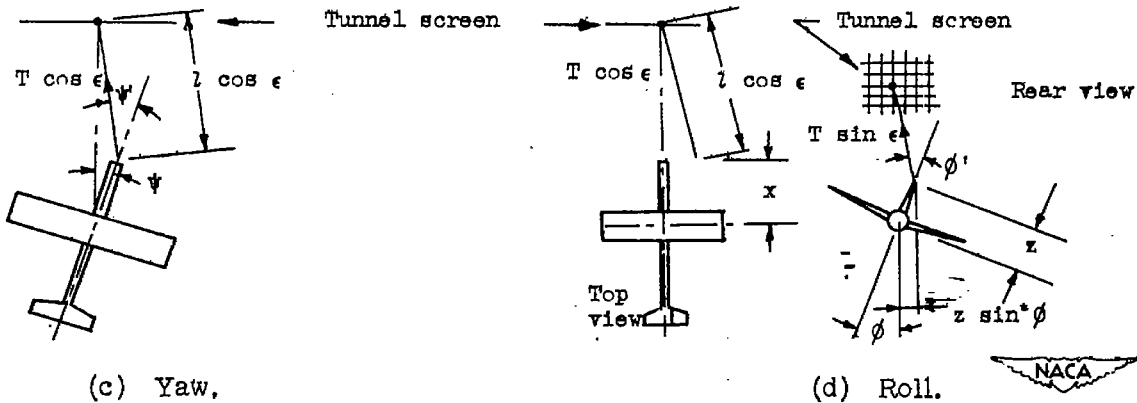
Figure 7.- Correlation of the period and the reciprocal of the time to damp to one-half amplitude of the lateral oscillations of the glider model at zero towline length as obtained from theory and tests for various values of $-C_{l\beta}$. (For other conditions see table II.)



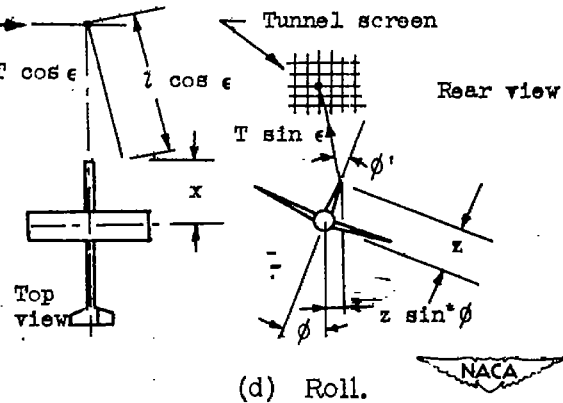
(a) Steady flight condition; $\epsilon = 0, y = 0$.



(b) Sidewise displacement.



(c) Yaw.



(d) Roll.



Figure 8.- Sketch showing the relationships used in obtaining the towline derivatives.